IEEE Photonics Journal
An IEEE Photonics Society Publication

Open Access

Design of Optimal Illumination Patterns in Single-Pixel Imaging Using Image Dictionaries

Volume 12, Number 4, August 2020

Jun Feng
Shuming Jiao
Yang Gao
Ting Lei
Luping Du

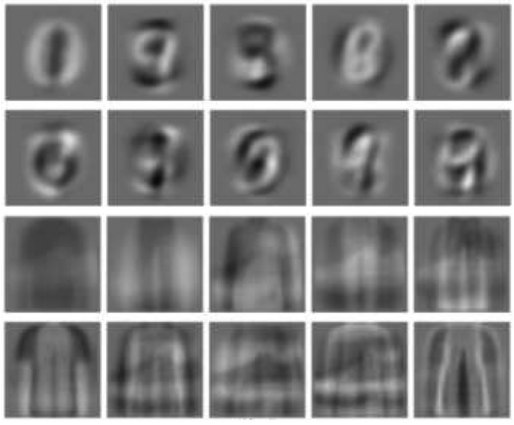

DOI: 10.1109/JPHOT.2020.3002477

IEEE photonics SOCIETY

IEEE

Design of Optimal Illumination Patterns in Single-Pixel Imaging Using Image Dictionaries

Jun Feng,[1] Shuming Jiao ,[2] Yang Gao,[1] Ting Lei ,[2] and Luping Du [2]

[1]Nanophotonics Research Center, Shenzhen Key Laboratory of Micro-Scale Optical Information Technology & College of Physics and Optoelectronic Engineering, Shenzhen University, Shenzhen 518060, China
[2]Nanophotonics Research Center, Shenzhen Key Laboratory of Micro-Scale Optical Information Technology & Institute of Microscale Optoelectronics, Shenzhen University, Shenzhen 518060, China

DOI:10.1109/JPHOT.2020.3002477

Manuscript received May 8, 2020; revised June 7, 2020; accepted June 11, 2020. Date of publication June 15, 2020; date of current version June 29, 2020. This work was supported by the National Natural Science Foundation of China under Grants 61805145 and 11774240. Corresponding author: Shuming Jiao (e-mail: albertjiaoee@126.com).

Abstract: A single-pixel imaging (SPI) system is often applied to a specific scenario. The target object images may belong to a specific category and have some common features. Fourier or Hadamard illumination patterns can be sub-optimal since they are fixed and non-adaptive. We propose a novel scheme for designing and optimizing the illumination patterns adaptively from an image dictionary by extracting the common features using principal component analysis (PCA), with enhanced imaging efficiency.

Index Terms: Single-Pixel imaging, principal component analysis, ghost imaging, illumination pattern, dictionary, optimization.

1. Introduction

Single-pixel imaging (SPI) [1], [2] is a novel computational imaging technique for recording an object image using a single-pixel detector without spatial resolution. SPI systems can be classified into two categories, i.e. active SPI systems originated from computational ghost imaging (CGI) [3] and passive SPI systems originated from single-pixel cameras [4]. In the former situation, a light modulator is placed near the light source to generate structured illumination patterns. In the latter situation, the light modulator is placed in the image plane. But the working mechanisms of both active and passive SPI are similar. In this work, SPI is mainly referred to active SPI. In conventional imaging, a two-dimensional object image is recorded at once by a pixelated image sensor array. In SPI, varying illumination patterns are projected onto the object sequentially and a single-pixel intensity sequence is recorded correspondingly. Mathematically, each single-pixel intensity value is the inner product between the object image and each illumination pattern. Finally the two-dimensional object image can be computationally reconstructed when both the recorded intensity sequence and the illumination patterns are known. A typical optical setup of SPI is shown in Fig. 1.

SPI can exhibit substantial advantages over conventional imaging under some circumstances, e.g. when the cost of pixelated image sensor is high for certain spectral bands, when no direct line

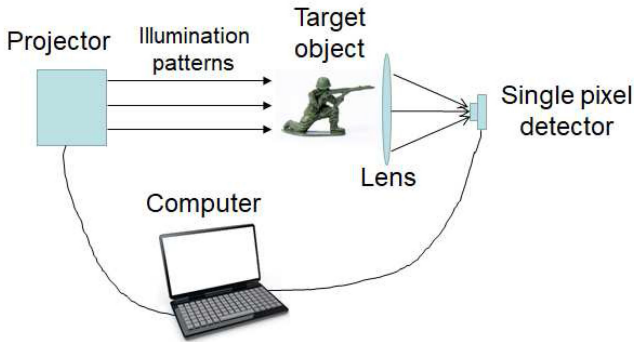

Fig. 1. Optical setup for a single-pixel imaging system.

of sight is available for the object scene or when the light condition is very weak. In previous works, SPI has been extensively investigated for various applications such as terahertz imaging [5], three dimensional (3-D) imaging [6], [7], microscopy [8], scattering imaging [9], optical security [10]–[12], and gas leak monitoring [13].

Despite the success, some challenges remain to be addressed for SPI systems. One inherent drawback of a SPI system is its low imaging efficiency and long image acquisition time. A reconstructed object image with reasonable quality can only be obtained when an adequate number of illuminations are sequentially projected and the corresponding single-pixel intensities are recorded by the detector. It will be favorable if a high-quality object image can be reconstructed using only a small number of illuminations. From the hardware aspect, a light modulation device [3], [14] with a higher refreshing rate for generating structured illumination can dramatically shorten the image acquisition time. For example, a LED array has a much higher refreshing rate than a conventional projector [14] but such hardware requires additional cost. In previous works, the imaging efficiency of SPI can also be improved from the computational aspects: optimized reconstruction algorithms and optimized illumination patterns. Compressive sensing [4], [15], [16] is one common reconstruction algorithm for random illumination patterns to achieve high-quality reconstruction at a low sampling ratio in SPI.

On the other hand, the imaging efficiency can be improved by designing proper basis illumination patterns such as Fourier transform sinusoidal patterns [17]–[22], Hadamard transform patterns [23]–[25], cosine transform patterns [26], and wavelet transform [27] patterns, instead of random intensity patterns. For a natural smooth image, the low frequency components in the transformed domain (e.g. Fourier transform, Hadamard transform, and cosine transform) account for most information. The object image can be approximately reconstructed from only the small number of single-pixel intensities corresponding to these low frequency components. Therefore a SPI with basis patterns can achieve the same imaging quality with a significantly reduced number of illuminations. In addition, the image reconstruction can usually be realized with a fast inverse orthogonal transform for basis-pattern illumination, instead of iterative optimization in compressive sensing.

2. Proposed Illumination Pattern Design Scheme for Single-Pixel Imaging Scheme

In many cases, a SPI system is usually applied to a specific scenario. The target object images may belong to a specific category and have some common features. The basis patterns in the previous schemes [17]–[27] are fixed for varying categories of target object images and hence the imaging efficiency is still sub-optimal. In this paper, optimized illumination patterns are designed for each

different category of object images adaptively by extracting the common image features from a pre-given image dictionary with the principal component analysis (PCA) algorithm. It shall be noticed that, the concept of image dictionary and the concept of PCA (or singular value decomposition, SVD) have already been attempted in previous SPI works [16], [28]. But these works [16], [28] focus on the optimal reconstruction algorithms when the illumination patterns are random intensity patterns in SPI. The illumination patterns in SPI can be optimized as one layer in the deep learning network but only modified Hadamard binary patterns can be obtained [29]. The illumination patterns can be optimized from sample images for object classification but it is not for real imaging [30]. In the previous work [31], the illumination patterns in SPI are designed from a dictionary under a compressive sensing framework, which requires some computational cost of iterative optimization for image reconstruction [32]. In comparison, a non-iterative inverse orthogonal-basis transform can be directly employed for image reconstruction in this work. Overall, an optimized basis-illumination pattern design scheme based on image dictionaries for SPI with PCA is proposed for the first time in this work.

It is assumed that the spatial resolution of each illumination pattern, or the total number of pixels, is $N = X \times Y$ (X and Y refer to the horizontal and vertical extent of each illumination pattern respectively). In fact, this resolution is identical to the object image resolution in the imaging model. In our proposed scheme, a number of exemplar object images (training images) need to be collected in advance to constitute an image dictionary for a specific imaging scenario. Then the optimal illumination patterns are designed based on the common features extracted from the image dictionaries and can be applied to any target object image similar to the exemplar images in the dictionary. It is assumed that totally M training images are used in the dictionary and each image is represented by a row vector of length N. A two dimensional matrix D with size $M \times N$ can be employed to represent all the training images. A normalized dictionary matrix A can be obtained after the average value of each column vector in D is subtracted from each element in the corresponding column. Then, the covariance matrix $A^T A$ with a size of $N \times N$ is calculated. A PCA [33]–[36], or SVD, can be performed on $A^T A$ to decompose the matrix into eigenvalues and eigenvectors. It is supposed that Q is the eigenvector matrix of $A^T A$ with size $N \times N$ (each row is an eigenvector). The eigenvectors (rows) in Q are arranged in the descending order of corresponding eigenvalues.

From a statistical point of view, PCA is a transform that converts a set of observations of M correlated variables into a weighted combination of N orthogonal uncorrelated basis variables (principal components). Here in our case, each variable is equivalent to an object image and each observation is equivalent to a pixel intensity in the image. PCA can perform data reduction since the first $K(1 \leq K \leq N)$ principal components (eigenvectors and eigenvalues) can account for most of the variability in the original M variables. In previous works, PCA has been extensively employed in data compression and dimension reduction applications [33]–[36].

Each row vector in Q is orthogonal to each other and all the row vectors are similar to the basis patterns in Fourier transform, Hadamard transform or other transforms. For a given object image, denoted by a column vector I with length N, the following transform can be performed given by Eq. (1) and a set of weighting coefficients $W = [w_1, w_2, w_3, \ldots, w_N]^T$ can be obtained.

$$W = QI \tag{1}$$

Each element in W is obtained by the inner product between the column vector I representing the object image and the row vector representing each principal component (or eigenvector basis pattern) $q_k(1 \leq k \leq N)$ in Q. This transform exactly matches with the SPI model. If q_k is employed as the illumination pattern, the weighting coefficient w_k can be recorded by the single-pixel detector. It shall be noticed that both the object image and illumination patterns are two-dimensional rather than a one-dimensional vector in a real SPI system and the 1D/2D conversion is a straightforward re-indexing. To achieve high imaging efficiency, only K most significant principal components (instead of all N ones) can be employed as the actual illumination patterns for SPI. For one target object image that does not belong to the image dictionary but has similar image characteristics to

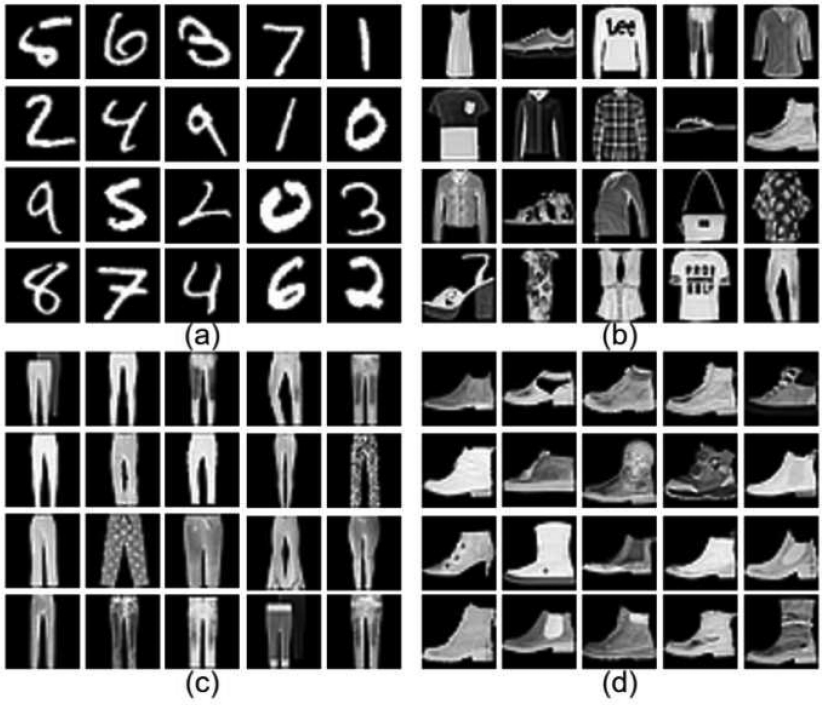

Fig. 2. Some examples in each category of training and testing images: (a) Number digit images from the MNIST dataset [37]; (b) Mixed fashion product images from the Fashion-MNIST dataset [38]; (c) Trousers images from the Fashion-MNIST dataset [38]; and (d) Boot images from the Fashion-MNIST dataset [38].

the training images, the acquired weighting coefficients for a small number of principal component patterns can already recover most image information. Finally, the target object image I can be computationally reconstructed from the acquired single-pixel intensity values (weighting coefficients) W and the corresponding illumination patterns Q by an inverse transform, similar to Fourier transform or Hadamard transform.

The pixel intensity values in the principal components can be both positive and negative. However, illumination patterns only allow positive pixel values in a practical optical system. So the pixel values need to be normalized first. For each normalized illumination pattern, both the original pattern and the complementary pattern will be projected. For example, one pixel has a normalized intensity 0.43 and its intensity will be $1 - 0.43 = 0.57$ in the complementary pattern. The final single-pixel intensity value is obtained by subtracting the single-pixel intensity value corresponding to the complementary pattern from the single-pixel intensity value corresponding to the original pattern.

3. Results and Discussion

In this work, four different categories of object images, including number digit images from the MNIST dataset [37], mixed fashion product images (consisting of ten sub-categories) from the Fashion-MNIST dataset [38], trousers images from the Fashion-MNIST dataset [38] and boot images from the Fashion-MNIST dataset [38] are assumed to be the original object images in SPI. Some examples of images belonging to each category are shown in Fig. 2. With the help of a coumputer which has a Matlab R2018b environment with Intel(R) Core(TM) i5-7200 U CPU (2.50 GHz) and 8 GB RAM, four different sets of illumination patterns are designed for each

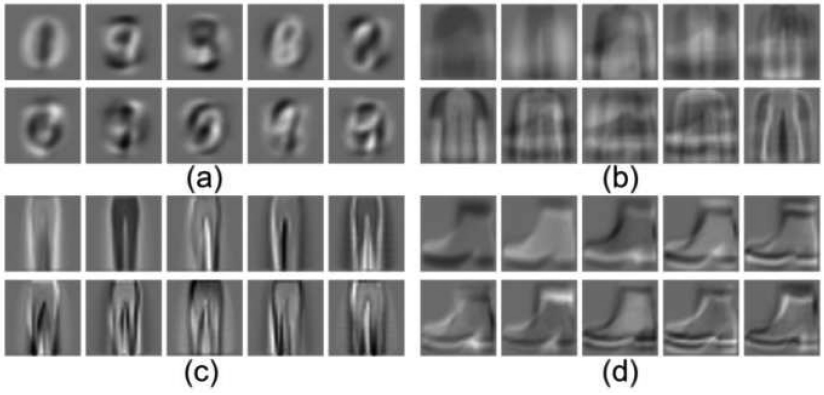

Fig. 3. First ten principal illumination patterns designed in our scheme for (a) Number digit images, (b) Mixed fashion product images, (c) Trousers images, and (d) Boot images.

TABLE I

Number of Training & Testing Images and Calculation Time for Designing the Illumination Patterns for Each Object Image Category in the Simulation

Category	Image Size	Number of training images	Calculation time for designing the illumination patterns	Number of testing images
Hand-written digit images	32×32	3000	0.848274s	100
Mixed fashion product images	32×32	1000	0.849660s	120
Trousers images	32×32	900	0.537023s	100
Boot images	32×32	980	0.370039s	120

category of object images correspondingly by extracting the principal components with our proposed scheme described above. The number of pixels in each object image and each illumination pattern is 32×32. The first ten optimized illumination patterns for each category are shown in Fig. 3 as examples. The number of training images and testing images taken from each category and the calculation time for designing the illumination patterns of each category are presented in Table 1. The results indicate that the amount of calculation time required to produce illumination patterns is acceptable and it may slightly increase as the number of training images increases.

In the simulation, the average quality of reconstructed testing images in the four categories with our proposed scheme is presented in Fig. 4. The results are compared with the conventional Fourier single-pixel imaging (FSPI) [17] and the conventional Hadamard single-pixel imaging (HSPI) [23]. In FSPI and HSPI, the illumination patterns are ordered from low-frequency components to high-frequency components in a zig-zag manner in the Fourier spectrum or Hadamard spectrum. To enhance the contrast of reconstructed images, the pixel values below a certain lower bound and above a certain upper bound are truncated.

It can be observed that the reconstruction results in our scheme have the highest Peak-Signal-to-Noise-Ratio (PSNR) values under the same number of illuminations compared with the ones in conventional FPSI and conventional HPSI especially at lower sampling ratios. The results in Fig. 4 indicate that our proposed scheme can yield better imaging efficiency than FSPI, and FSPI generally has better imaging efficiency than HSPI. Compared with our proposed PCA scheme, FSPI and HSPI have an advantage of being free of pre-known image dictionaries. In addition, HSPI only requires a binary light modulation device. Some examples of reconstructed images at different sampling ratios with these three schemes are demonstrated in Fig. 5. The results in Fig. 5 visually reveal the fact that the visual quality of reconstructed object images in our proposed

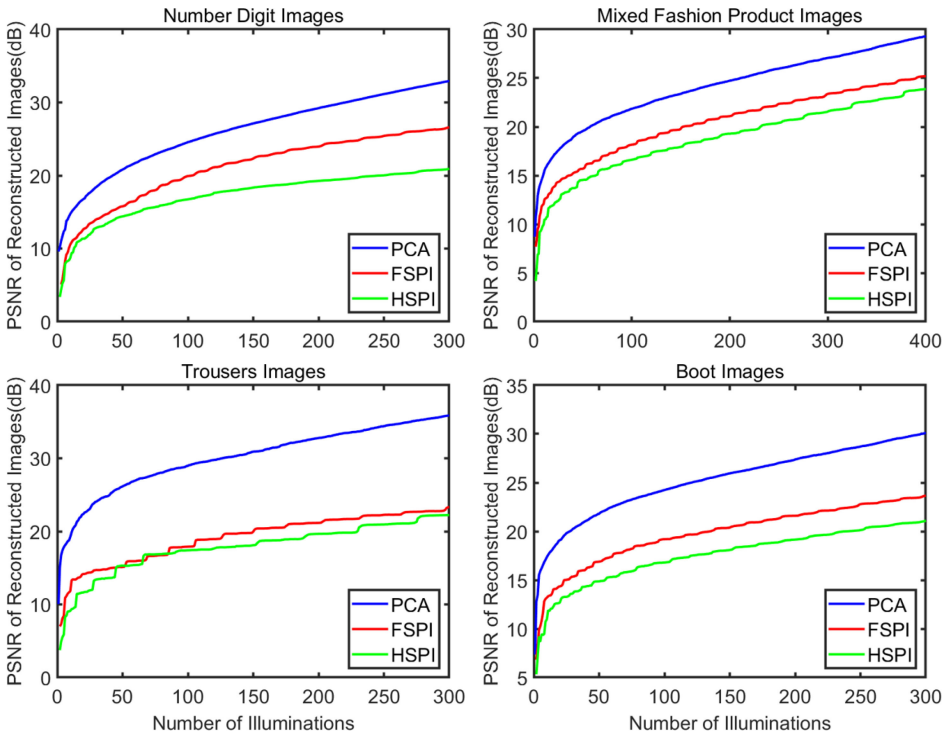

Fig. 4. Average image quality (PSNR) of simulated reconstructed results in SPI with our proposed PCA scheme (blue), conventional FSPI (red) and conventional HSPI (green): (a) Number digit images; (b) Mixed fashion product images; (c) Trousers images; and (d) Boot images.

scheme is superior to the ones in FSPI and HSPI. When the number of illuminations is small (e.g. less than 100), the reconstructed images in FSPI and HSPI are usually heavily blurred but the reconstructed images already show acceptable quality in our proposed PCA scheme. The advantage of our proposed scheme is more evident for the last two categories compared with the first two categories. This is because there are more common features among the images in the last two categories than the ones in the mixed number or mixed fashion product category. The performance of our proposed scheme depends on the degree of similarity between the images in the specific imaging scenario.

The number of training images will affect the final imaging efficiency in our proposed scheme. Generally, the imaging efficiency will increase as the number of training samples increases, shown in Fig. 6. The reason is that more diversified training samples will contain more comprehensive features for a specific image category. But the improvement of imaging efficiency will be minor if the number of training samples reaches a certain level. It is necessary that the test images and the training images belong to the same category in our scheme. When the training images and testing images are mismatched (e.g. MNIST training images and Fashion-MNIST testing images), it can be observed that the reconstructed image has much degraded quality in Fig. 7. The results show that our proposed scheme has a limitation that a training image dictionary consistent with the actual target test image has to be available in advance.

Optical experiments are conducted to verify the performance of our proposed scheme as well. The optical setup is shown in Fig. 8, which is the same as the one in the previous work [30]. A paper card with printed object image is illuminated by the patterns projected from a JmGO G3 projector. The single-pixel intensity values are recorded by a Thorlabs FDS1010 photodiode detector. The reconstruction results with our proposed scheme and conventional FSPI from the experimentally recorded data are shown in Fig. 9. The experimental results basically agree with the simulated results, with some extra noise contamination.

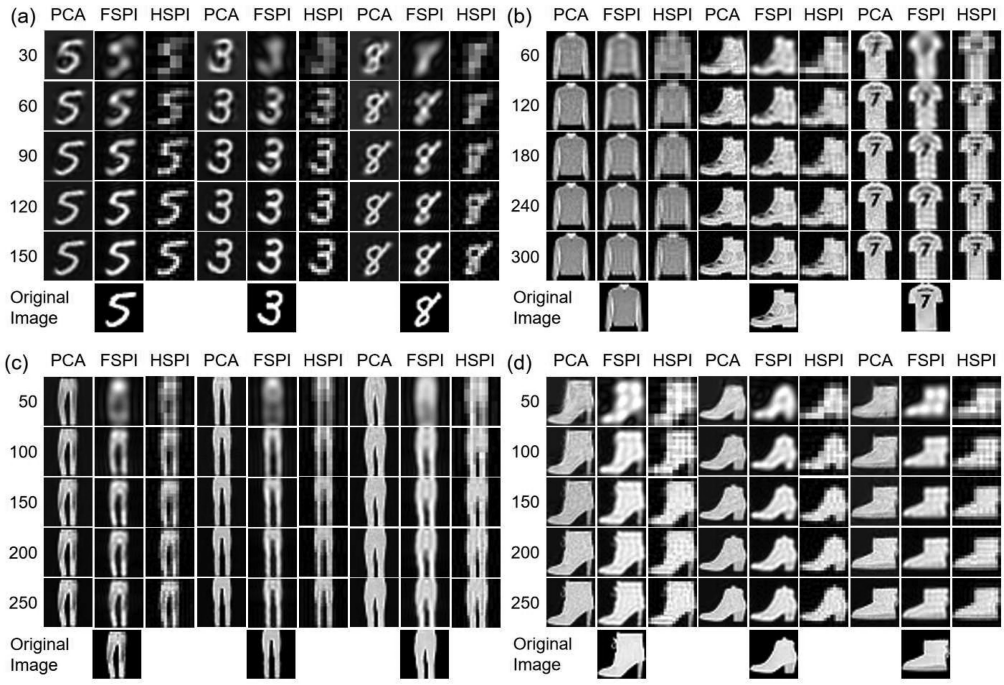

Fig. 5. Simulated reconstructed test images for each category of images in SPI with our proposed scheme (PCA), conventional FSPI and conventional HSPI for varying number of illuminations (denoted by the row index): (a) Number digit images; (b) Mixed fashion product images; (c) Trousers images; and (d) Boot images.

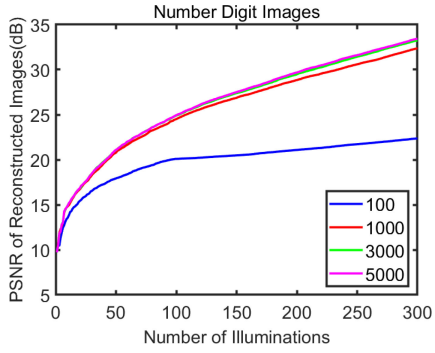

Fig. 6. Average image quality (PSNR) of simulated reconstructed results for number digit images in SPI with 100 training images (blue), 1000 training images (red), 3000 training images (green), and 5000 training images (purple).

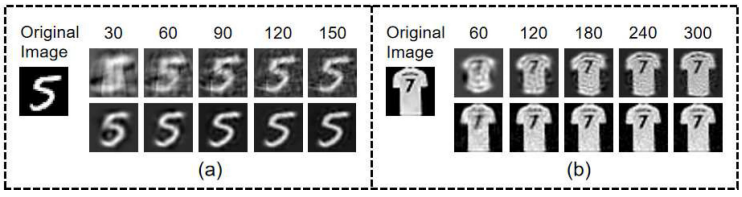

Fig. 7. Simulated reconstruction results in SPI with a mismatched (top row) or matched (bottom row) training category with our proposed scheme (PCA): (a) Number digit images, (b) Mixed fashion product images.

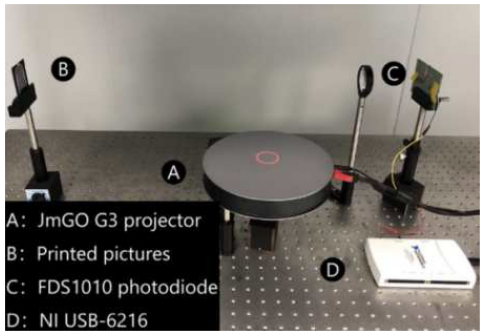

Fig. 8. Optical setup of our SPI experiment [30].

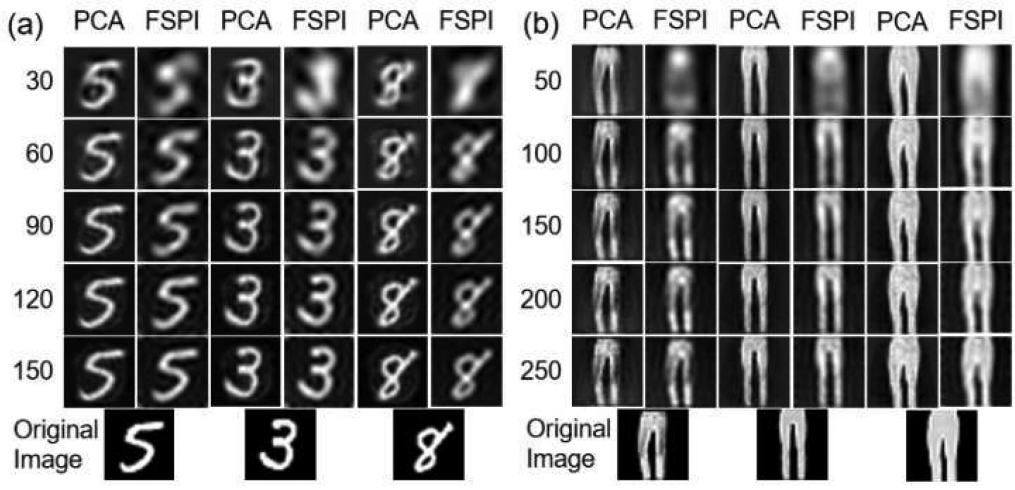

Fig. 9. Experimental reconstruction results for two image categories in SPI with our proposed scheme (PCA) and conventional FSPI for varying number of illuminations: (a) Number digit images; (b) Trousers images.

4. Conclusion

In summary, an optimized illumination pattern design scheme in single-pixel imaging (SPI) based on image dictionaries and principal component analysis (PCA) is proposed. Compared with conventional fixed and non-adaptive basis patterns (e.g. Fourier patterns), the orthogonal basis patterns are adaptively optimized based on the common features of training images. Simulated and experimental results show that our proposed scheme can achieve better imaging quality than the conventional FSPI and HSPI scheme under the same sampling ratio.

Acknowledgment

The authors wish to thank the anonymous reviewers for their valuable suggestions.

References

[1] M. P. Edgar, G. M. Gibson, and M. J. Padgett, "Principles and prospects for single-pixel imaging," *Nature Photon.*, vol. 13, no. 1, pp. 13–20, 2019.
[2] M.-J. Sun and J.-M. Zhang, "Single-pixel imaging and its application in three-dimensional reconstruction: A brief review," *Sensors*, vol. 19, no. 3, p. 732, 2019.

[3] J. H. Shapiro, "Computational ghost imaging," *Phys. Rev. A*, vol. 78, no. 6, 2008, Art. no. 061802.
[4] M. F. Duarte *et al.*, "Single-pixel imaging via compressive sampling," *IEEE Signal Process. Mag.*, vol. 25, no. 2, pp. 83–91, Mar. 2008.
[5] W. L. Chan, K. Charan, D. Takhar, K. F. Kelly, R. G. Baraniuk, and D. M. Mittleman, "A single-pixel terahertz imaging system based on compressed sensing," *Appl. Phys. Lett.*, vol. 93, no. 12, 2008, Art. no. 121105.
[6] B. Sun *et al.*, "3D computational imaging with single-pixel detectors," *Science.*, vol. 340, no. 6134, pp. 844–847, 2013.
[7] M. Sun *et al.*, "Single-pixel three-dimensional imaging with time-based depth resolution," *Nature Commun.*, vol. 7, no. 1, 2016, Art. no. 12010.
[8] N. Radwell, K. J. Mitchell, G. M. Gibson, M. P. Edgar, R. Bowman, and M. J. Padgett, "Single-Pixel infrared and visible microscope," *Optica*, vol. 1, no. 5, pp. 285–289, 2014.
[9] E. Tajahuerce *et al.*, "Image transmission through dynamic scattering media by single-pixel photodetection," *Opt. Express*, vol. 22, no. 14, pp. 16 945–16 955, 2014.
[10] Z. Zhang, S. Jiao, M. Yao, X. Li, and J. Zhong, "Secured single-pixel broadcast imaging," *Opt. Express*, vol. 26, no. 11, pp. 14 578–14 591, 2018.
[11] W. Chen and X. Chen, "Object authentication in computational ghost imaging with the realizations less than 5% of nyquist limit," *Opt. Lett.*, vol. 38, no. 4, pp. 546–548, 2013.
[12] S. Jiao, J. Feng, Y. Gao, T. Lei, and X. Yuan, "Visual cryptography in single-pixel imaging," *Opt. Express*, vol. 28, no. 5, pp. 7301–7313, 2020.
[13] G. M. Gibson *et al.*, "Real-time imaging of methane gas leaks using a single-pixel camera," *Opt. Express*, vol. 25, no. 4, pp. 2998–3005, 2017.
[14] Z.-H. Xu, W. Chen, J. Penuelas, M. Padgett, and M.-J. Sun, "1000 fps computational ghost imaging using LED-based structured illumination," *Opt. Express*, vol. 26, no. 3, pp. 2427–2434, 2018.
[15] L. Bian, J. Suo, Q. Dai, and F. Chen, "Experimental comparison of single-pixel imaging algorithms," *J. Opt. Soc. America A*, vol. 35, no. 1, pp. 78–87, 2018.
[16] X. Hu, J. Suo, T. Yue, L. Bian, and Q. Dai, "Patch-primitive driven compressive ghost imaging," *Opt. Express*, vol. 23, no. 9, pp. 11 092–11 104, 2015.
[17] Z. Zhang, X. Ma, and J. Zhong, "Single-pixel imaging by means of fourier spectrum acquisition," *Nature Commun.*, vol. 6, no. 1, 2015, Art. no. 6225.
[18] K. M. Czajkowski, A. Pastuszczak, and R. Kotyński, "Real-time single-pixel video imaging with Fourier domain regularization," *Opt. Express*, vol. 26, no. 16, pp. 20 009–20 022, 2018.
[19] J. Huang, D. Shi, K. Yuan, S. Hu, and Y. Wang, "Computational-weighted Fourier single-pixel imaging via binary illumination," *Opt. Express*, vol. 26, no. 13, pp. 16 547–16 559, 2018.
[20] W. Meng, D. Shi, J. Huang, K. Yuan, Y. Wang, and C. Fan, "Sparse Fourier single-pixel imaging," *Opt. Express*, vol. 27, no. 22, pp. 31 490–31 503, 2019.
[21] K. Zhang *et al.*, "Fourier single-pixel imaging based on lateral inhibition for low-contrast scenes," *IEEE Photon. J.*, vol. 11, no. 5, Oct. 2019, Art. no. 6901711.
[22] Y. Xiao, L. Zhou, and W. Chen, "Fourier spectrum retrieval in single-pixel imaging," *IEEE Photon. J.*, vol. 11, no. 2, Apr. 2019, Art. no. 7800411.
[23] L. Wang and S. Zhao, "Fast reconstructed and high-quality ghost imaging with fast Walsh–Hadamard transform," *Photon. Res.*, vol. 4, no. 6, pp. 240–244, 2016.
[24] Y. Xiao, L. Zhou, and W. Chen, "Direct single-step measurement of hadamard spectrum using single-pixel optical detection," *IEEE Photon. Technol. Lett.*, vol. 31, no. 11, pp. 845–848, Jun. 2019.
[25] M. Sun, L. Meng, M. P. Edgar, M. J. Padgett, and N. Radwell, "A Russian Dolls ordering of the Hadamard basis for compressive single-pixel imaging," *Scientific Rep.*, vol. 7, no. 1, pp. 1–7, 2017.
[26] B. Liu, Z. Yang, X. Liu, and L. Wu, "Coloured computational imaging with single-pixel detectors based on a 2D discrete cosine transform," *J. Modern Opt.*, vol. 64, no. 3, pp. 259–264, 2017.
[27] W. Yu, M. Li, X. Yao, X. Liu, L. Wu, and G. Zhai, "Adaptive compressive ghost imaging based on wavelet trees and sparse representation," *Opt. Express*, vol. 22, no. 6, pp. 7133–7144, 2014.
[28] X. Zhang *et al.*, "Singular value decomposition ghost imaging," *Opt. Express*, vol. 26, no. 10, pp. 12 948–12 958, 2018.
[29] C. F. Higham, R. Murray-Smith, M. J. Padgett, and M. P. Edgar, "Deep learning for real-time single-pixel video," *Scientific Rep.*, vol. 8, no. 1, pp. 1–9, 2018.
[30] S. Jiao, J. Feng, Y. Gao, T. Lei, Z. Xie, and X. Yuan, "Optical machine learning with incoherent light and a single-pixel detector," *Opt. Lett.*, vol. 44, no. 21, pp. 5186–5189, 2019.
[31] C. Hu, Z. Tong, Z. Liu, Z. Huang, J. Wang, and S. Han, "Optimization of light fields in ghost imaging using dictionary learning," *Opt. Express*, vol. 27, no. 20, pp. 28 734–28 749, 2019.
[32] S. Sun *et al.*, "Ghost imaging normalized by second-order coherence," *Opt. Lett.*, vol. 44, no. 24, pp. 5993–5996, 2019.
[33] H. Abdi and L. J. Williams, "Principal component analysis," *Wiley Interdisciplinary Rev.: Comput. Statist.*, vol. 2, no. 4, pp. 433–459, 2010.
[34] S. Jiao, Z. Zhuang, and W. Zou, "Fast computer generated hologram calculation with a mini look-up table incorporated with radial symmetric interpolation," *Opt. Express*, vol. 25, no. 1, pp. 112–123, 2017.
[35] C. Zuo, Q. Chen, W. Qu, and A. Asundi, "Phase aberration compensation in digital holographic microscopy based on principal component analysis," *Opt. Lett.*, vol. 38, no. 10, pp. 1724–1726, 2013.
[36] S. Yeom, B. Javidi, P. Ferraro, D. Alfieri, S. DeNicola, and A. Finizio, "Three-dimensional color object visualization and recognition using multi-wavelength computational holography," *Opt. Express*, vol. 15, no. 15, pp. 9394–9402, 2007.
[37] L. Deng, "The MNIST database of handwritten digit images for machine learning research [best of the web]," *IEEE Signal Process. Mag.*, vol. 29, no. 6, pp. 141–142, Nov. 2012.
[38] H. Xiao, K. Rasul, and R. Vollgraf, "Fashion-MNIST: A novel image dataset for benchmarking machine learning algorithms," 2017, *arXiv:1708.07747*.